

Chiral-Plasmon-Tuned Potentials for Atom Trapping at the Nanoscale

Zhao Chen, Fan Zhang, Xueke Duan, Tiancai Zhang, Qihuang Gong, and Ying Gu*

Neutral atom trapping is of importance in precision quantum metrology and quantum information processing where the atom can be viewed as an excellent frequency reference. However, creating tunable optical traps compatible with the optical nanostructures is still a challenge. Here, by introducing the chiroptical effects of a plasmonic structure into atom trapping, an active tunable potential for 3D stable optical trapping at the nanoscale is demonstrated. By altering the incident light from left- to right-handed circularly polarized, the tunable range of position and potential of the trapped atoms can reach ≈ 60 nm and $\approx 0.51N$ mK (N denotes input power with unit mW), respectively. In addition, the blue-detuned circularly polarized light guarantees the ultralow scattering rate and ultralong trapping lifetime. The trap centers are about hundreds of nanometers away from the structure surface, which ensures the stability of the trapping system due to the ignorable surface potential. This chiral-based tunable atom trapping system broadens the application of chiral metamaterials and has important impact on all-optical modulation, atomic on-chip integration, manipulation of cold atoms, and quantum many-body systems.

1. Introduction

Trapping and optically interfacing neutral atoms in the near field of nanophotonic structures are essential requirements for their use in advanced quantum technologies, e.g., precision quantum metrology and quantum information processing.^[1,2] There are in general three ways for neutral atoms trapping, including radiation-pressure traps,^[3] magnetic traps,^[4] and

optical dipole traps.^[5] Among them, optical dipole traps, which primarily use the gradient forces of the incident light to push atoms into a potential dip, has become a widely used tool because the trapping mechanism is independent of the particular sublevel of the electronic ground state of the trapped atoms.^[5] For the blue-detuned traps,^[6–8] generally, the atoms are trapped in the local potential minima, then the photon scattering rates are very low, while the experimental setup is usually more complicated. In contrast, for the red-detuned traps, although the trapping system is very compact, for example, the focusing systems,^[9,10] the trapped atoms will be subjected to obvious atomic coherence and heating effect^[5] since the atoms will be attracted to the position with the largest intensity of light.

Miniaturization and integration of photonic devices is an important trend in the future development. Recently, optical


nanofibers are increasingly being used in cold atom experiments due to their versatility and the clear advantages when developing all-fibered systems for quantum technologies.^[11–17] However, two-color (a red- and a blue-detuned light) or multi-color traps are needed in the nanofiber system to form a stable trapping because of the attractive van der Waals forces,^[12–17] which undoubtedly increase the complexity of the structure and the difficulty of the experiments. To address these problems, researchers combine the atom trapping with plasmonic nanostructures which are in a subwavelength scale with great local field enhancement effects,^[18,19] achieving surface plasmon polariton (SPP)-based atom trapping systems.^[20–23] Later, a stable 3D atom trapping was achieved based on single blue-detuned light in an array of plasmonic nanoholes.^[24] These SPP-based atom trapping systems have many advantages, e.g., the structures are compact and easy for expansion and atomic on-chip integration, the resulting potential traps are small enough to trap single atom. Nevertheless, it is difficult to actively tailor the position and the potential of the trapped atoms, which is of great significance in atom-atom interactions and resonance fluorescence.^[25,26] Therefore, a stable atom trapping nanosystem that is adjustable by external means is urgently needed.

Chiroptical effects are characterized by different optical responses for right- and left-handed circularly polarized light (RCP and LCP).^[27,28] Attaining strong chiroptical effects has great significance for applications in biomolecules and chemical

Dr. Z. Chen, Dr. F. Zhang, Dr. X. Duan, Prof. Q. Gong, Prof. Y. Gu
State Key Laboratory for Mesoscopic Physics
Collaborative Innovation Center of Quantum Matter
Department of Physics
Peking University
Beijing 100871, China
E-mail: ygu@pku.edu.cn

Prof. T. Zhang, Prof. Q. Gong, Prof. Y. Gu
Collaborative Innovation Center of Extreme Optics
Shanxi University
Taiyuan, Shanxi 030006, China

Prof. T. Zhang
State Key Laboratory of Quantum Optics and Quantum Optics Devices
Institute of Opto-Electronics
Shanxi University
Taiyuan 030006, China

 The ORCID identification number(s) for the author(s) of this article can be found under <https://doi.org/10.1002/adom.201800261>.

DOI: 10.1002/adom.201800261

reagent detection.^[28,29] The optical chirality is extremely weak in nature media. As a solution, researchers have focused on studying chiral metamaterials, due to their ability to enhance the chiroptical effects by several orders of magnitude.^[27,30,31] This external adjustment by RCP and LCP of the electromagnetic field, makes chiral metamaterials highly promising potential applications including negative refractive index materials,^[32–34] ultrasensitive biosensing,^[27,35,36] and broadband circular polarized devices.^[37–39] Moreover, because surface plasmon resonances can offer strong near-field enhancement to increase chirality in metamaterial, numerous designs based on plasmonic building blocks,^[30] such as gammadion shape meta-atom,^[33,40,41] L-shapes,^[42–44] twisted-arc shape,^[45–47] nanoslits, and nanohole arrays^[48–50] are proposed. In spite of wide applications have been achieved by chiral metamaterials,^[32–39] creating tunable optical traps for neutral atoms compatible with chiral metamaterials has never been reported.

In this paper, we introduce the planar chiral plasmonic metamaterial structure into neutral atom trapping, e.g., ⁸⁷Rb trapping. Simulation results show that the position and the potential of the trapped atoms can be easily tuned by altering the phase difference of the components of incident light from LCP to RCP. The tunable range of position and potential of the trapped atoms is ≈ 60 nm and ≈ 0.51 nK due to the different near-field scattering intensities. The designed structure consists of an array of two four-vertical slits as planar chiral metamaterial at visible wavelengths, whose resonant field can be used as a blue-detuned laser light for atom trapping. A blue-detuned circularly polarized light ensures the 3D traps for ⁸⁷Rb atoms with ultralow scattering rates. The trap centers are about hundreds of nanometers away from the structure surface at resonance, which guarantees the stability of the trapping system. This type of atom trapping, based on modulation of LCP and RCP, provides a promising possibility for atomic on-chip integration, all-optical modulation, and manipulation of cold atoms, which will have great significance in nanophotonics and quantum computation.

2. Designed Chiral-Plasmon Structure

As illustrated in Figure 1a, the chiral plasmonic structure consists of an array of nanoslits etched in $h = 150$ nm thin silver layer on $d = 200$ nm thin silica (SiO₂) substrate. The pink dashed line shows the unit cell of the presented arrays and the geometrical parameter symbols. In order to better illustrate the chiral response, each unit cell is made of two four-vertical nanoslits of identical length L and width w separated by different gaps g and g' . The structure is periodic in x - and y -directions, while only a single layer is considered in z -direction.

Periodic arrays of subwavelength slits in metallic films exhibits an extraordinary optical transmission effect.^[19] Here, the transmission of CP at normal incidence from the backside is investigated by the commercial software COMSOL Multiphysics. The period P_x , P_y , length L , width w , different gaps g and g' are 1400, 700, 300, 100, 10, and 50 nm, respectively. The refractive index of SiO₂ is $n = 1.45$ and the relative permittivity of silver is taken from ref. [51]. The electric field components of incident CP light are set as $E_x = e^{-j\omega t}$, $E_y = e^{-j\omega t + j\theta}$, and $E_z = 0$ [ω denotes the frequency of the incident light, θ represents the phase difference, $\theta = \pi/2$ or $3\pi/2$ corresponding to RCP or LCP]. The calculated transmission spectra for RCP (black curve) and LCP (red curve) incidences are shown in Figure 1b. It is clearly observed that the same resonant peak appears at $\lambda = 748$ nm with different transmission efficiencies, about 0.42 and 0.53 for RCP and LCP incidences, respectively. The circular state of polarization is perfectly preserved in the transmitted wave, with a conversion ratio less than 1.5% between RCP and LCP (Figure S1, Supporting Information). The difference in transmittance of LCP and RCP is usually called circular dichroism,^[49,50] which is a typical feature of a chiral response (see Figure S2a in the Supporting Information). The appearance of the circular dichroism spectrum can be attributed to the Ohmic loss of the silver (results from the imaginary part of the permittivity), which is confirmed by the simulation of the metamaterial made from an ideal metal (see Figure S2b in the Supporting

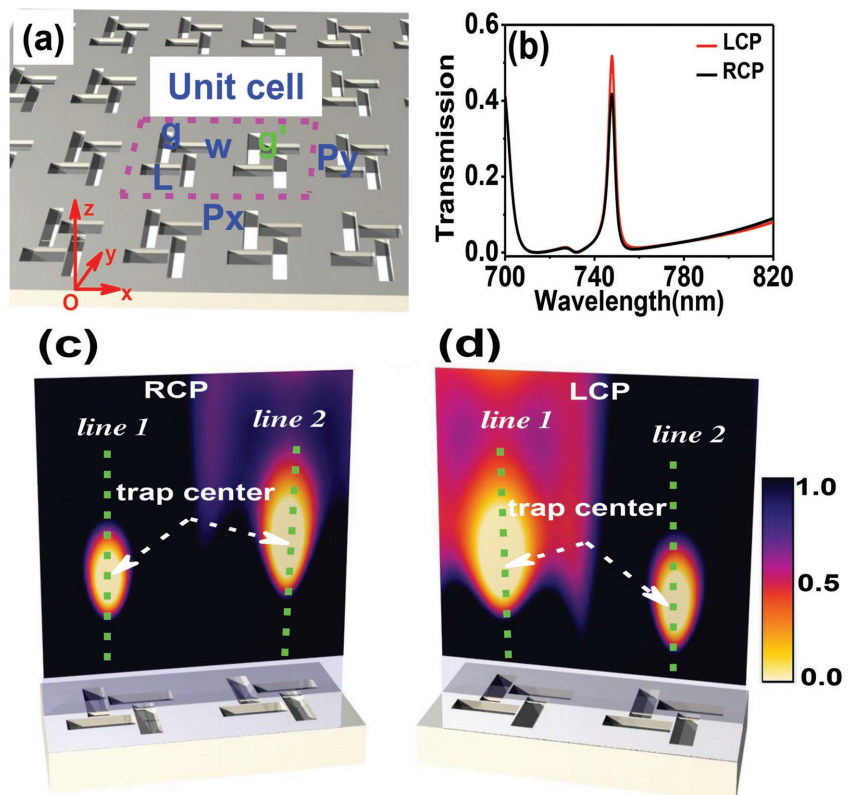


Figure 1. a) Schematic of the array of nanoslits in a metallic film. The pink dashed line shows the unit cell of the presented arrays and the main geometrical parameter symbols. b) Simulation results of the normalized zero-order transmission spectrum for RCP (black curve) and LCP (red curve) incidences. Normalized spatial electric field intensity $|E|^2$ distributions for c) RCP and d) LCP excitations at $\lambda = 748$ nm for one unit cell.

Information). In other words, the Ohmic loss plays a significant role in the observed chiroptical effect.^[43,52]

The difference in transmission efficiency between RCP and LCP means different electric field distributions at resonance ($\lambda = 748$ nm) and also implies tunable electric field intensity. At this point, we consider this difference of such fields on tunable atom trapping. In order to better understand the proposed system's advantages in atom trapping, we plot the spatial electric field intensity $|E|^2$ distributions of the system at $\lambda = 748$ nm, which are shown in Figure 1c,d at RCP and LCP excitations, respectively. Obviously, two trap centers (local electric field minima) appear at each plot, which are both about hundreds of nanometers away from the structure surface. The appearance of these trap centers can be attributed to the near-field scattering of light by periodic plasmonic nanoslits.^[20,24] Herein, the electric field E is the superposition of the evanescent (SPPs) and the spatial electric field through the nanoslits. The local electric field minima suggests the blue-detuned optical trap for neutral atom manipulation. A neutral atom, e.g., ^{87}Rb atom, can be trapped in the local electric field minima via optical dipole forces with blue-detuned light.^[5] Here, the resonant wavelength $\lambda = 748$ nm is selected to be blue-detuned to the D2 line of ^{87}Rb , which repels the atoms from the high light intensity due to the optical dipole forces to the minimum.

As we know, a neutral atom (atomic state i with Zeeman level m_i) interacting with an electric field E experiences an optical dipole potential given by^[5]

$$U_{\text{opt}} = -\frac{1}{4}\alpha|E|^2 \quad (1)$$

Here, α is a reduced polarizability and its expression is taken from refs. [7,24]. For $\lambda = 748$ nm, the calculated polarizability is $\alpha \approx -5.07 \times 10^{-38}$ F m² for ^{87}Rb atoms. Therefore, the dipole potentials can be obtained according to the electric field intensity distributions. In addition, the trapped atoms will be subjected to the surface potential U_{sur} of the structure.^[12–17] Therefore, the total potential U_{tot} experienced by the trapped atoms is the sum of the attractive U_{sur} and repulsive U_{opt}

$$U_{\text{tot}} = U_{\text{opt}} + U_{\text{sur}} \quad (2)$$

However, the trap centers are both about hundreds of nanometers away from the surface, so the U_{sur} can be negligible relative to U_{opt} in our calculations.^[53] Thus, in this text, we use U_{opt} instead of U_{tot} to represent the total potential of the trapped atom. In addition, the scattering rate and trapping lifetime of the trapped atoms are the two important indexes for the viability of an atom trapping system. Trapped atoms meet with the photon scattering, which will result in a momentum recoil, and then can lead to atoms loss.^[5] For ^{87}Rb atom in a dipole trap, we can assume that the major contributions to the scattering rates, Γ_{sc} , are from the dipole transition rates from ground state $S_{1/2}$ to the excited states $P_{1/2}$ and $P_{3/2}$.^[54,55] Each scattered photon contributes some recoil energy to the atom, which will lead to a loss of atoms from the dipole trap. Thus, the scattering rates Γ_{sc} and a trap lifetime τ_c are given as

$$\Gamma_{\text{sc}} = \left(\frac{\Gamma_{1/2}}{3\Delta_{1/2}} + \frac{2\Gamma_{3/2}}{3\Delta_{3/2}} \right) \frac{U_{\text{opt}}}{\hbar} \quad (3)$$

$$\tau_c = \frac{U_{\text{eff}}}{2R^r\Gamma_{\text{sc}}} \quad (4)$$

where $\Gamma_{1/2}$ and $\Gamma_{3/2}$ are the dipole transition matrix elements from the ground state $S_{1/2}$ to the excited states $P_{1/2}$ and $P_{3/2}$, respectively, \hbar is the reduced Planck's constant, Δ is the detuning, $R^r = 2\pi^2\hbar^2/(m\lambda^2)$ is the recoil energy associated with a blue photon, and m is the atomic mass of ^{87}Rb , respectively. Therefore, in order to achieve a better stable trapping system, we hope to obtain the trapped atoms with ultralow scattering rate and ultralong trapping lifetime, which has great significance in reducing the atom detecting errors.

3. Chiral-Plasmon-Tuned Potentials for ^{87}Rb Atom Trapping

To illustrate the trapping characteristics of the proposed structure quantitatively, we calculate the optical dipole potential U_{opt} distributions along line 1 and line 2 (denoted by green dashed lines in Figure 1c,d), shown in Figure 2. Here, the incident optical power is set as $P_0 = 1$ mW. $\Delta s/\Delta s'$ and $\Delta\text{trap}/\Delta\text{trap}'$ denote the movable position and tunable potential ranges of trapped atoms by altering the phase difference θ , respectively (s expresses the distance between trap center and the nanostructure surface). We define the effective trap depth U_{eff} as the potential difference between the potential minimum that the trapped ^{87}Rb atoms can escape and the potential of the trap center.^[24] Thus, the absolute value of $|U_{\text{eff-RCP}} - U_{\text{eff-LCP}}|$ is the potential tunable factor. This is because the tunable range of potential is proportional to the input power P_0 . Namely, we assume the incident power $P_0 = N$ mW, the tunable range of nanopotential is $\Delta\text{trap} = N \times |U_{\text{eff-RCP}} - U_{\text{eff-LCP}}|$ with the unit mK.

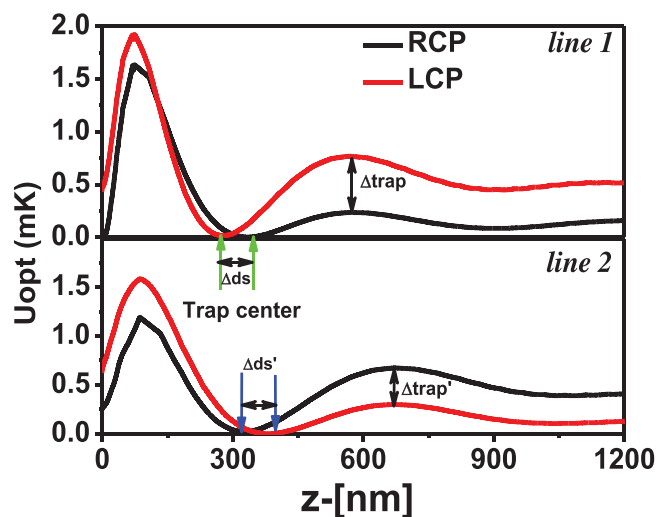


Figure 2. Corresponding optical dipole potential U_{opt} distributions along line 1 and line 2 (denoted by green dashed lines in Figure 1c,d) with $g = 10$ nm and $g' = 50$ nm for RCP and LCP excitations at $\lambda = 748$ nm.

Table 1. The concerned calculation results of the atom trapping system. Incident power P_0 , distance between trap center and structure surface ds , effective trap depth U_{eff} , scattering rate Γ_{sc} , and trapping lifetime τ_c .

	$P_0 = 1 \text{ mW}$	$ds \text{ [nm]}$	$U_{\text{eff}} \text{ [mK]}$	$\Gamma_{\text{sc}} \text{ [s}^{-1}\text{]}$	$\tau_c \text{ [s]}$
Line 1	RCP	390	0.24	0.1	6779
	LCP	326	0.75	0.7	3026
Line 2	RCP	323	0.65	1.0	1836
	LCP	382	0.30	0.1	8475

For expedient comparison, the concerned calculation results of the proposed structure on atom trapping are listed in **Table 1**. From the Table 1, it is found that $\Delta ds = 64 \text{ nm}$ (from 326 to 390 nm), $\Delta ds' = 59 \text{ nm}$ (from 323 to 382 nm) and $\Delta \text{trap} = 0.51N \text{ mK}$, $\Delta \text{trap}' = 0.35N \text{ mK}$. For a fixed input power ($P_0 = 1 \text{ mW}$), the achieved effective trap depth is only 1/6 and 1/80 mK in refs.[7] and,[56] respectively. Ultralow input power can effectively reduce the heating effect on atoms and increase the trapping lifetime. In addition, the scattering rate and the trapping lifetime are much more superior compared to previous reports.[54,55] Ultralow scattering rate and ultralong trapping lifetime have great significance in reducing the atoms detecting errors.

Furthermore, although the tunable potential range increase not significantly, the position range has increased nearly 20 times compared with single four-vertical nanoslits (see Figure S3 in the Supporting Information for details). Namely, we can tune the position of the trapped atoms by only changing the phase difference θ . The dynamic changing situation of the trap centers (trapped atoms) is displayed in the Supporting Information-II. It can be clearly seen that the trapping centers are moving back and forth at the conversion process by altering the phase difference θ . The realization of two different trap centers in the same unit cell has never been reported before, and each trap center can be effectively tuned by controlling the phase difference θ of incident light. The ability to tune neutral atoms at subwavelength scale would enable precision manipulation of atoms which is very important for quantum network capabilities and large-scale quantum communications.

Successively, we investigated the influence of parameters variations on the distributions of the optical dipole potentials along the line 1 and line 2 in Figure 1c,d. Herein, the calculated distributions of U_{opt} with different filled materials n (1.00) and n' (1.00, 1.10, 1.20) in one unit cell at resonance ($\lambda = 756 \text{ nm}$) for RCP and LCP excitations is displayed in **Figure 3** (the situation of U_{opt} with different gaps g (g') is shown in Figure S4

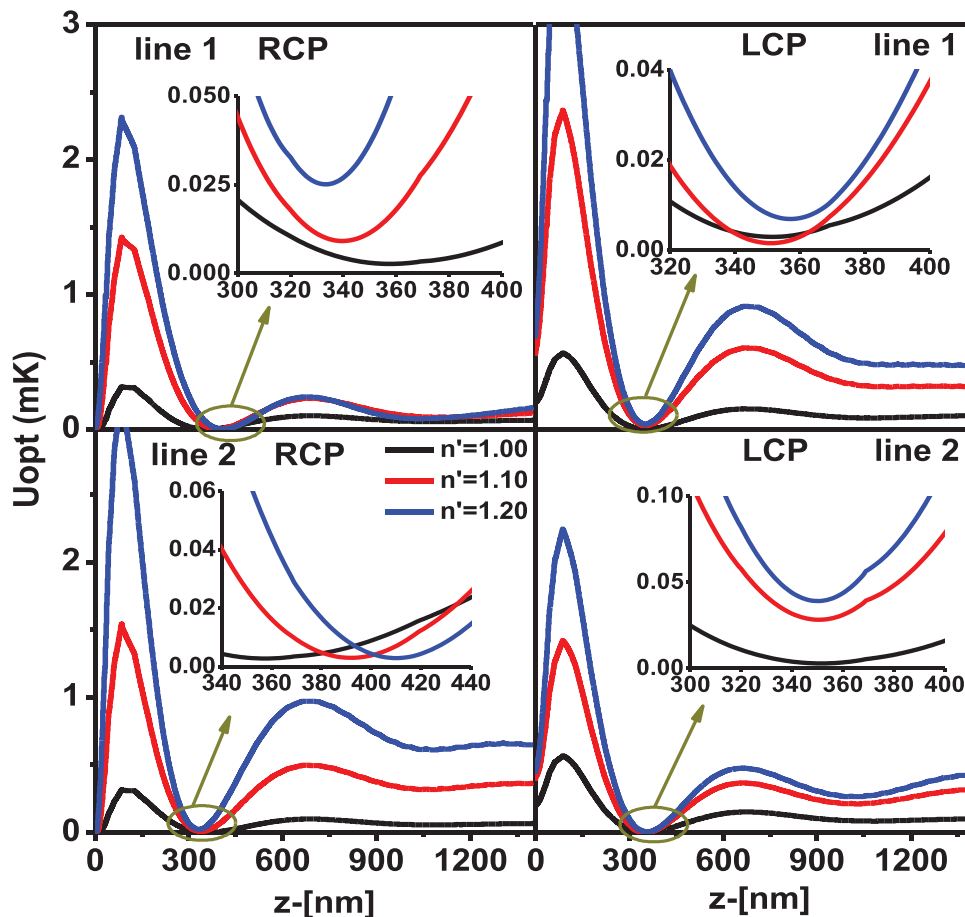


Figure 3. Influence of parameters variations on the distributions of the optical dipole potentials along the center line with different filled materials n (1.00) and n' (1.00, 1.10, 1.20) at $\lambda = 756 \text{ nm}$ for RCP and LCP incidences. The parameters are set as $P_x = 1400 \text{ nm}$, $P_y = 700 \text{ nm}$, $L = 300 \text{ nm}$, $w = 100 \text{ nm}$, and $g = g' = 10 \text{ nm}$.

in the Supporting Information). The insets show the enlarged trapping positions, and we can clearly see the tunable ranges of trapped atoms, which can be attributed to the different intensities of the near-field scattering. Moreover, it is found that when the system is at resonance ($n = 1.00$, $n' = 1.20$, $\lambda = 756$ nm), the U_{eff} is almost the largest, no matter RCP or LCP light incidences. The above results can offer us one of the ideas of constructing an atom trapping, which is to optimize the parameters to make the system resonant, and this will result in a maximum effective trap depth and the lowest scattering rate. In addition, the filled materials can be Kerr nonlinear materials, and the refractive index can be controlled by another beam of light, e.g., pumb light, which greatly increase the system's usability in all-optical manipulation.

Based on above analysis, we know that the use of external means by LCP and RCP provides us a new method of adjusting the atom trapping potential. In addition, this approach also provides the possibility for atomic on chip integration and large-scale atom array manipulation, which is required for many-body interaction, quantum computation, multibit quantum information, and quantum simulation. Further, by designing chiral structures with larger circular dichroism spectrum, such as the trapping wavelength is on resonance at RCP, suppressing resonance at LCP or conversely, a wider range of regulation of atom potential can be achieved.

4. Conclusion

In conclusion, we have demonstrated a chiral-plasmon-tuned 3D atom trapping independent of the surface potential that can be achieved in a single-layer planar chiral metamaterial at the nanoscale. The position and the potentials of the trapped atom can be easily tuned by altering the phase difference of the incident light. Meanwhile, the trapped atoms will move back and forth. The resonant field of the structure is used as the blue-detuned trapping light for neutral atoms, which greatly reduces the optical power, thanks to the excitation of SPPs. The trap centers are about hundreds of nanometers away from the structure surface, which arises from the near-field scattering of the periodic property. Our structure is easily fabricated and on-chip integrated. This chiral-based tunable atom trapping system broadens the application of chiral metamaterials and has important impact on all-optical modulation, atomic on-chip integration, and quantum information processing.

Supporting Information

Supporting Information is available from the Wiley Online Library or from the author.

Acknowledgements

This work was supported by the National Key R&D Program of China (Grant No. 2018YFB1107200), the National Natural Science Foundation of China (NSFC) (Grant Nos. 11704013, 11525414, 11634008, 11734001), and the China Postdoctoral Science Foundation under Grant No. 2017M620493.

Conflict of Interest

The authors declare no conflict of interest.

Keywords

atom trapping, chiral response, nanophotonics, plasmonic metamaterials

Received: February 27, 2018

Published online:

- [1] J. M. Morrissey, K. Deasy, M. Frawley, R. Kumar, E. Prel, L. Russell, V. G. Truong, S. N. Chormaic, *Sensors* **2013**, *13*, 10449.
- [2] J. D. Thompson, T. G. Tiecke, N. P. Leon, J. Feist, A. V. Akimov, M. Gullans, A. S. Zibrov, V. Vuletic, M. D. Lukin, *Science* **2013**, *340*, 1202.
- [3] E. L. Raab, M. Prentiss, S. Chu, D. E. Pritchard, *Phys. Rev. Lett.* **1987**, *59*, 2631.
- [4] J. Fortagh, C. Zimmermann, *Rev. Mod. Phys.* **2007**, *79*, 235.
- [5] R. Grimm, M. Weidemüller, *Adv. At. Mol. Opt. Phys.* **2000**, *42*, 1.
- [6] M. J. Piotrowicz, M. Lichtman, K. Maller, G. Li, S. Zhang, L. Isenhower, M. Saffman, *Phys. Rev. A* **2013**, *88*, 013420.
- [7] P. Zemanek, C. J. Foot, *Opt. Commun.* **1998**, *146*, 119.
- [8] N. T. Phuong Lan, D. T. Thuy Nga, N. A. Viet, *J. Phys.: Conf. Ser.* **2015**, *627*, 012017.
- [9] S. Kato, S. Chonan, T. Aoki, *Opt. Lett.* **2014**, *39*, 773.
- [10] P. F. Zhang, G. Li, T. C. Zhang, *J. Phys. B: At. Mol. Opt. Phys.* **2017**, *50*, 045005.
- [11] T. Nieddu, V. Gokhroo, S. N. Chormaic, *J. Opt.* **2016**, *18*, 053001.
- [12] N. V. Corzo, B. Gouraud, A. Chandra, A. Goban, A. S. Sheremet, D. V. Kupriyanov, J. Laurat, *Phys. Rev. Lett.* **2016**, *117*, 133603.
- [13] X. Qi, B. Q. Baragiola, P. S. Jessen, I. H. Deutsch, *Phys. Rev. A* **2016**, *93*, 023817.
- [14] A. Goban, K. S. Choi, D. J. Alton, D. Ding, C. Lacroute, M. Pototschnig, T. Thiele, *Phys. Rev. Lett.* **2012**, *109*, 033603.
- [15] E. Vetsch, D. Reitz, G. Sague, R. Schmidt, S. T. Dawkins, A. Rauschenbeutel, *Phys. Rev. Lett.* **2010**, *104*, 203603.
- [16] V. I. Balykin, K. Hakuta, F. Le Kien, J. Q. Liang, M. Morinaga, *Phys. Rev. A* **2004**, *70*, 011401 (R).
- [17] F. Le Kien, V. I. Balykin, K. Hakuta, *Phys. Rev. A* **2004**, *70*, 011401.
- [18] W. L. Barnes, A. Dereux, T. W. Ebbesen, *Nature* **2003**, *424*, 824.
- [19] T. W. Ebbesen, H. J. Lezec, H. Ghaemi, T. Thio, P. A. Wolf, *Nature* **1998**, *391*, 667.
- [20] D. E. Chang, J. D. Thompson, H. Park, V. Vuletic, A. S. Zibrov, P. Zoller, M. D. Lukin, *Phys. Rev. Lett.* **2009**, *103*, 123004.
- [21] B. Murphy, L. V. Hau, *Phys. Rev. Lett.* **2009**, *102*, 033003.
- [22] M. Gullans, T. Tiecke, D. E. Chang, J. Feist, J. Thompson, J. Cirac, P. Zoller, M. D. Lukin, *Phys. Rev. Lett.* **2012**, *109*, 235309.
- [23] C. Garcia-Segundo, H. Yan, M. S. Zhan, *Phys. Rev. A* **2007**, *75*, 030902.
- [24] Z. Chen, F. Zhang, Q. Zhang, J. Ren, H. Hao, X. Duan, P. Zhang, T. Zhang, Y. Gu, Q. Gong, *Photonics Res.* **2017**, *5*, 436.
- [25] A. Gonzalez, C. Hung, D. E. Chang, J. Cirac, H. Kimble, *Nat. Photonics* **2015**, *9*, 320.
- [26] H. Tamura, T. Unakami, J. He, Y. Miyamoto, K. Nakagawa, *Opt. Express* **2016**, *24*, 8132.
- [27] A. Ben-Moshe, B. M. Maoz, A. O. Govorov, G. Markovich, *Chem. Soc. Rev.* **2013**, *42*, 7028.
- [28] M. Schäferling, *Chiral Nanophotonics*, Springer International Publishing, Cham, Switzerland **2017**.
- [29] M. Hentschel, M. Schäferling, X. Duan, H. Giessen, N. Liu, *Sci. Adv.* **2017**, *3*, e1602735.

- [30] V. K. Valev, J. J. Baumberg, C. Sibia, T. Verbiest, *Adv. Mater.* **2013**, 25, 2517.
- [31] X. Wang, Z. Tang, *Small* **2017**, 13, 1601115.
- [32] S. Zhang, Y. S. Park, J. Li, X. Lu, W. Zhang, X. Zhang, *Phys. Rev. Lett.* **2009**, 102, 023901.
- [33] M. Kuwata-Gonokami, N. Saito, Y. Ino, M. Kauranen, K. Jefimovs, T. Vallius, T. Jari, Y. Svirko, *Phys. Rev. Lett.* **2005**, 95, 227401.
- [34] A. S. Karimullah, C. Jack, R. Tullius, V. M. Rotello, G. Cooke, N. Gadegaard, L. D. Barron, M. Kadodwala, *Adv. Mater.* **2015**, 27, 5610.
- [35] Z. Wang, Y. Wang, G. Adamo, B. The, Q. Wu, J. Teng, H. Sun, *Adv. Opt. Mater.* **2016**, 4, 883.
- [36] F. Lu, Y. Tian, M. Liu, D. Su, H. Zhang, A. O. Govorov, O. Gang, *Nano Lett.* **2013**, 13, 3145.
- [37] W. Li, Z. J. Coppens, L. V. Besteiro, W. Wang, A. O. Govorov, J. Valentine, *Nat. Commun.* **2015**, 6, 8379.
- [38] Y. Zhao, M. A. Belkin, A. Alu, *Nat. Commun.* **2012**, 3, 870.
- [39] Y. Zhao, A. Alu, *Nano Lett.* **2013**, 13, 1086.
- [40] R. Zhao, L. Zhang, J. Zhou, T. Koschny, C. M. Soukoulis, *Phys. Rev. B* **2011**, 83, 035105.
- [41] J. Zhou, D. R. Chowdhury, R. Zhao, A. K. Azad, H. Chen, C. M. Soukoulis, A. J. Taylor, J. F. Ohara, *Phys. Rev. B* **2012**, 86, 035448.
- [42] C. Helgert, E. Pshenay-Severin, M. Falkner, C. Menzel, C. Rockstuhl, E. B. Kley, A. Tunermann, F. Lederer, T. Pertsch, *Nano Lett.* **2011**, 11, 4400.
- [43] W. Ye, X. Yuan, C. Guo, J. Zhang, B. Yang, S. Zhang, *Phys. Rev. Appl.* **2017**, 7, 054003.
- [44] M. Li, Q. Zhang, F. Qin, Z. Liu, Y. Piao, Y. Wang, J. Xiao, *J. Opt.* **2017**, 19, 075101.
- [45] Y. Cui, L. Kang, S. Lan, S. Rodrigues, W. Cai, *Nano Lett.* **2014**, 14, 1021.
- [46] E. Plum, J. Zhou, J. Dong, V. A. Fedotov, T. Koschny, C. Soukoulis, N. I. Zheludev, *Phys. Rev. B* **2009**, 79, 035407.
- [47] B. Maoz, A. B. Moshe, D. Vestler, O. Bar-Elli, G. Markovich, *Nano Lett.* **2012**, 12, 2357.
- [48] E. Hendry, R. V. Mikhaylovskiy, L. D. Barron, M. Kadpdwala, T. J. Davis, *Nano Lett.* **2012**, 12, 3640.
- [49] A. B. Khanikaev, N. Arju, Z. Fan, D. Purtseladze, F. Lu, J. Lee, P. Sarriugarte, M. Schnell, R. Hillenbrand, M. A. Belkin, G. Shvets, *Nat. Commun.* **2016**, 7, 12045.
- [50] B. Frank, X. Yin, M. Schaferling, J. Zhao, S. M. Hein, P. V. Braun, H. Giessen, *ACS Nano* **2013**, 7, 6321.
- [51] P. B. Johson, R. W. Christy, *Phys. Rev. B* **1972**, 6, 4370.
- [52] Z. Li, M. Gokkavas, E. Ozbay, *Adv. Opt. Mater.* **2013**, 1, 482.
- [53] D. E. Chang, K. Sinha, J. M. Taylor, H. J. Kimble, *Nat. Commun.* **2014**, 5, 4343.
- [54] M. Daly, V. G. Truong, C. F. Phelan, K. Deasy, S. N. Chormaic, *New J. Phys.* **2014**, 16, 053052.
- [55] J. P. Burke, S. Chu, G. Bryant, C. J. Williams, P. S. Julienne, *Phys. Rev. A* **2002**, 65, 043411.
- [56] P. Xu, X. He, J. Wang, M. Zhan, *Opt. Lett.* **2010**, 35, 2164.